Elastic waves in random-fibre networks

1997 J. Phys. A: Math. Gen. 30 6601

(http://iopscience.iop.org/0305-4470/30/19/004)

J. Phys. A: Math. Gen. **30** (1997) 6601–6613. Printed in the UK PII: S0305-4470(97)79706-3

Elastic waves in random-fibre networks

J Åström, M Kellomäki and J Timonen

Department of Physics, University of Jyväskylä, PO Box 35, FIN-40351 Jyväskylä, Finland

Received 15 November 1996, in final form 12 June 1997

Abstract. The propagation of the first displacement maximum of a semi-infinite wavetrain in a two-dimensional random-fibre network is analysed. Model calculations and numerical simulations are used for demonstrating that two qualitatively different wavefront velocities appear in the network. A transient wave, which travels fast and whose amplitude decreases exponentially, dominates the short-time behaviour when the bending stiffness of the fibres is small and the driving frequency is high. This mode can be described by a one-dimensional model. The transient-wave mode propagates even if the bending stiffness of the fibres vanishes, in which case the normal sound velocity is zero. The usual, and slower, effective medium mode always dominates at late times. It also dominates at short times if the driving frequency is low and/or the bending stiffness of the fibres is relatively high.

1. Introduction

A model material built of randomly deposited fibres which are connected at intersections, is an interesting object for research. The technological applications of such a model are numerous. For example, it can contribute to the understanding of common materials such as glass fibres, polymers and ordinary paper. Random fibre networks are also interesting from an academic point of view, as, in contrast with the extensively used randomized lattice models [1], they contain disorder in a natural way. It is therefore easier to compare numerical and theoretical results with experiment.

Earlier investigations of random-fibre networks have mainly focused on the network stiffness and quasistatic fracture [2–7]. These investigations have all been based on the effective medium model introduced by Cox [2]. The Cox model predicts correctly the average stress distribution along the fibres, and the average stress in a fibre, as a function of orientation and with respect to the direction of the external stress [6]. The Cox model can also be extended to model fracture, and it gives valuable qualitative insight into the fracture of random-fibre networks [5, 6, 8]. The Cox model is not, however, capable of giving quantitatively correct results for the mechanical properties of fibre networks [7] (like Young's modulus or strength). The Cox model fails in particular close to the percolation critical density, and if, for example, the bending stiffness of the fibres become so small that stress can only be transferred as elongation of the fibres [5, 7, 9].

In this paper we investigate the propagation of the leading elastic wavefront through a random-fibre network. By the leading wavefront we mean here the first displacement maximum through the fibre crossing points of the network. We apply the Cox model formula of the network stiffness to calculate the sound velocity. The result is consistent with numerical simulations in the case of low frequencies and a high bending stiffness of the fibres. For a low bending stiffness and/or high frequency, the Cox model result

0305-4470/97/196601+13$19.50

fails, however. In this case the propagation of the first displacement maximum is correctly described by a one-dimensional model. A cross over between the two model solutions is observed when the frequency and/or the bending stiffness of the fibres are changed. A similar cross over is also seen in the amplitude decay. Simulations reveal a power-law decay in the Cox model limit and an exponential decay in the one-dimensional model limit.

To illustrate random-fibre networks and the two model solutions, we show in figure 1 two networks for which the effective medium model and the one-dimensional model, respectively, are valid. In figure 1(a) a snapshot is taken of a network after the first quarter of a transverse wave has entered the network. The wavelength is long, and the network obviously deforms very much like a continous and homogeneous medium. The square in this figure denotes the original boundaries of the network. In figure 1(b) no deformations are shown as the amplitude decays very rapidly in this case when the one-dimensional model is valid. Instead a circle is drawn around those fibre–fibre crossings which have been reached by the highest average velocities of a longitudinal wave (i.e. a threshold value is chosen for the distance of each crossing from the left edge of the network divided by the time of arrival of the first displacement maximum). These points form more or less one-dimensional paths. To further demonstrate the difference between these two networks, the amplitude (A) of the first displacement maximum at each crossing is plotted in figure 2 as a function of the distance (x) from the left edge of the network. The driving amplitude is in both cases 0.01. The amplitude remains more or less constant in the network of figure 1(a), while it decreases more or less exponentially in the network of figure 1(b) (these two behaviours appear as two distinct branches in figure 2).

2. The numerical model

A great deal of the results reported in this paper are based on the numerical model used to produce figure 1. It is a model of an elastic random-fibre network obeying Newton's equations of motion. Geometrically a network is constructed by randomly placing equally long line segments (fibres of length L) on a square of size $L_x \times L_y$. At every point where two fibres cross they are assumed to be rigidly bonded to each other. The midpoints and the orientations of the fibres are chosen from uniform uncorrelated distributions. The orientation angles are chosen from the interval $-\pi/2$ to $\pi/2$. The midpoints are uniformly scattered over a square of width $(L_x + L)$ and height $(L_y + L)$. The midpoints of the fibres are thus allowed to fall outside the square used in the simulations to avoid the density of the fibres to be lower at the boundaries. In order to apply Newton's mechanics to the network, distribution of the mass must be defined. For numerical efficiency we have lumped all the mass of the network on the interfibre crossings. For simplicity we further assume that there is a mass point of equal size (m) at each crossing point. This model corresponds to the case when the 'glue' which connects the fibres is heavy compared to the fibre-mass density. The boundary conditions are chosen such that the fibre ends at the boundaries are free to move without constraints (i.e. 'free' boundary conditions), except at the left boundary ($x = 0$) where the fibre ends are forced to move in either the x or the y direction, giving rise to predominantly longitudinal or transverse waves, respectively. The forced motion of these fibre ends is described by a semi-infinite sine wave $\sin(\omega t)$ for $t \geqslant 0$, which means that the first displacement maximum leaves the left boundary at $t = \pi/2\omega$.

The network is set to be at rest at the time $t = 0$, and the displacements and the accelerations of all the mass points in the network are calculated iteratively at discrete time

(*a*)

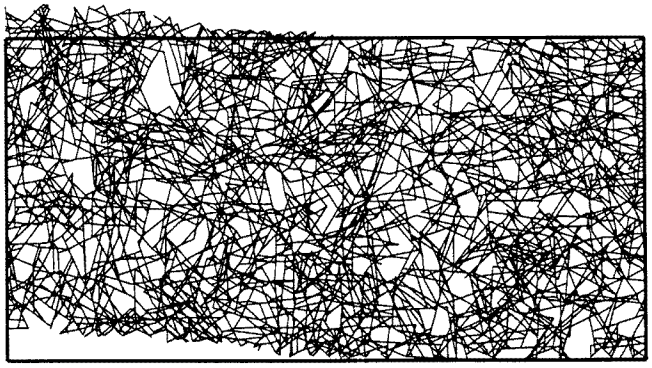

(*b*)

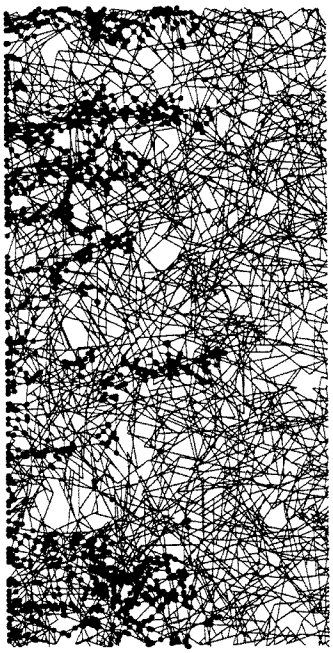

Figure 1. (*a*) The displacements at $t = \pi/2\omega$ in a network with $q/q_c = 6$, $m = 0.01$, $w = 0.15$; transverse wave with a frequency of 0.0125. (*b*) A network with $q/q_c = 6$, $m = 0.12$, $w = 0.2$. Circles mark the interfibre crossings which have been reached by the first displacement maximum. The more or less one-dimensional paths formed by the circles are the fastest paths of propagation in the network. The frequency is 0.125.

steps using a discretized form of Newton's equations of motion, i.e.

$$\frac{M}{\Delta t^2}U(t+\Delta t) = \left[\frac{2M}{\Delta t^2} - K\right]U(t) - \frac{M}{\Delta t^2}U(t-\Delta t) \tag{1}$$

where M is a diagonal matrix containing the masses, K is the global stiffness matrix of the

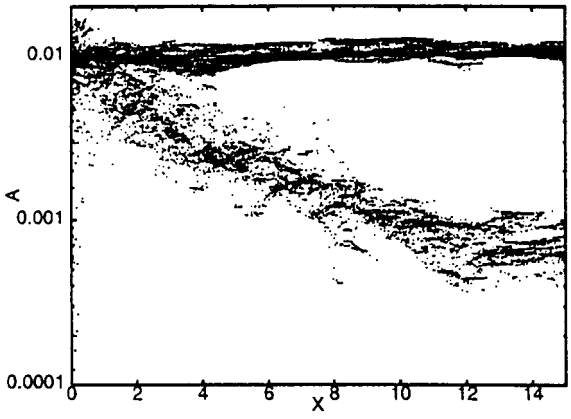

Figure 2. The amplitudes (A) of the first displacement maxima in two different networks which have the same parameters as those in figure 1. A is plotted as a function of distance x from the driving source. The data corresponding to figure 1(a) give an almost constant amplitude, while those corresponding to figure 1(b) describe a more or less exponentially decaying amplitude.

network, $U(t)$ is a time-dependent vector containing the displacements of the mass points, and Δt is the length of the time step. For each single-fibre segment (between two adjacent fibre crossings) we use the stiffness matrix of a slender linear elastic beam,

$$k = \begin{pmatrix} \frac{EA}{l} & 0 & 0 & \frac{-EA}{l} & 0 & 0 \\ 0 & \frac{12EI}{l^3} & \frac{6EI}{l^2} & 0 & \frac{-12EI}{l^3} & \frac{6EI}{l^2} \\ 0 & \frac{6EI}{l^2} & \frac{4EI}{l} & 0 & \frac{-6EI}{l^2} & \frac{2EI}{l} \\ \frac{-EA}{l} & 0 & 0 & \frac{EA}{l} & 0 & 0 \\ 0 & \frac{-12EI}{l^3} & \frac{-6EI}{l^2} & 0 & \frac{12EI}{l^3} & \frac{-6EI}{l^2} \\ 0 & \frac{6EI}{l^2} & \frac{4EI}{l} & 0 & \frac{-6EI}{l^2} & \frac{2EI}{l} \end{pmatrix} \tag{2}$$

where $A = w^2$ is the cross-section area of the fibres, l the length of the segment, E Young's modulus and $I = w^4/12$ the moment of inertia; k is given here in the local coordinate system of a fibre (i.e. the x axis along the fibre axis). The six diagonal elements of k correspond to the x and y displacements and rotation of the left and the right end of the fibre segment, respectively. K is constructed by transforming the k of all segments into the global coordinate system and then summing them together (a lot of rows and columns containing only zeros must of course be added to equation (2) before the summation is made). Note that K is not updated as the network is being deformed. That is, in a strict sense our model is only correct for infinitesimal deformations. In particular, collisions between adjacent fibres due to deformation are completely neglected. We follow the propagation of the first displacement maximum by recording it at each mass point. To filter numerical noise we use a lower cut-off on the displacement amplitude such that amplitudes lower than this limit are not accepted as first-displacement maxima.

3. The one-dimensional model

The one-dimensional model describes the wave propagation velocity and the amplitude decay in a case when either the bending or the axial stiffness of the fibres is small in comparison with the other. In these limits we model the network as an ensemble of random, one-dimensional chains of fibre segments (segments of fibres between two crossing points).

This ensemble of segment chains consists of all possible paths along the fibres which lead across the network in the x direction (i.e. the wave-propagation direction). Every segment belongs, of course, to many possible paths, but since the first displacement maxima of the induced elastic waves (which we consider here) are dominated by signals travelling along the shortest routes, we can neglect all long paths. When the density is relatively high (i.e. not close to the critical density of percolation), the shorter paths are relatively straight, and they do not cross each other very often. This means that, if the average bending stiffness of the fibre segments is much smaller than their average axial stiffness, we can, in the first approximation, neglect interactions between these paths. The case of induced transverse waves can be described by a similar model in the limit of large bending stiffness. In both these limits there will be no time for stress relaxation in the y direction. For short wavelengths the first displacement maximum can then be considered as travelling along an ensemble of random *non-interacting* chains of fibre segments. The equations of motion for such a chain are just discrete one-dimensional classical wave equations with a varying stiffness constant [10, 11]. The variation in the stiffness constant comes from the random variations in the length of the segments. The equations of motions are simply given by

$$m\ddot{u}_i - k_i(u_{i+1} - u_i) + k_{i-1}(u_i - u_{i-1}) = 0 \tag{3}$$

where $u_{i+1} - u_i$ is the strain of the fibre segment separating the points $i + 1$ and i in the chain. When a longitudinal wave propagates along a chain, fibre segments will be deformed through elongation and compression. We can then use the axial modulus or the element $(1, 1)$ in the stiffness matrix (equation (2)) for k_i, i.e. $k_i = Ew^2/l_i$, where l_i is the length of segment i. If, on the other hand, a transverse wave propagates along the chain, fibre segments will deform through shear and bending. If the moment of inertia of the crossings is relatively high, we can simply use the matrix element $(2, 2)$ in equation (2) for k_i, i.e. $k_i = (w/l_i)^2 Ew^2/l_i$ for the transverse waves. Notice, however, that there are no perfectly straight chains in a random-fibre network (cf figure 1), which means that fibre segments belonging to a chain will be deformed in all possible ways. The first displacement maximum will, however, always be dominated by the fastest of the modes. If $u(x)$ varies slowly in comparison with all segment lengths, then equation (3) can be replaced by an effective differential equation. If there would be no variations in the segment lengths, the continuum limit of equation (3) would simply be a classical wave equation

$$m\frac{\mathrm{d}^2u}{\mathrm{d}t^2} - kl^2\frac{\mathrm{d}^2u}{\mathrm{d}x^2} = 0. \tag{4}$$

In the case of longitudinal waves (i.e. when $k_i = Ew^2/l_i$), it is easy to show that the continuum limit of equation (3) is similar to equation (4). We only have to replace l with $l(x) = (l_i + l_{i-1})/2$, and k with $k(x) = Ew^2/l(x)$. The local velocity given by equation (4) is $v(x) = l(x)\sqrt{k(x)/m}$. By integrating over the distribution of the segment lengths $l(x)$ we get the average velocity of longitudinal waves.

The segment-length distribution in a network with a high fibre density is similar to the cluster-size distribution of one-dimensional percolation. This distribution is easily shown to be a simple exponential distribution

$$P(l) = (2q/\pi L)\exp(-2ql/\pi L) \tag{5}$$

where q is the fibre density defined as the average number of fibres in an area of size L^2 [12].

For transverse waves the situation is more complicated. If we write l_i as $\hat{l}_i - \delta l$, and l_{i-1} as $\hat{l}_i + \delta l$, it is, however, straightforward to show that the continuum limit of equation (3) can be written in the form

$$m\frac{\mathrm{d}^2u}{\mathrm{d}t^2} - k(x)l^2(x)(1+\eta_1)\frac{\mathrm{d}^2u}{\mathrm{d}x^2} - k(x)l^2(x)\eta_2\frac{\mathrm{d}u}{\mathrm{d}x} = 0 \tag{6}$$

where $\eta_1 = (\delta l/l(x))^2[3 - (\delta l/l(x))^2]/[1 - (\delta l/l(x))^2]^2$, and $\eta_2 = (4\delta l/l(x))/[1 - (\delta l/l(x))^2]^2$. For high frequencies, or when η_2 is small, it can be shown using the Fourier transform [13] that η_2 only causes random fluctuations in the amplitude but does not affect the velocity. For low frequencies we expect that η_2, which describes small-scale random fluctuations around zero, will only cause temporal perturbations in the profile of the wave. That is, we expect that the effect of η_2 on the velocity can be neglected. This means that equation (6) is simply a wave equation of the same form as equation (4). The velocity of transverse waves can thus be obtained by integrating over the distributions of $l(x)$ and δl. Carrying out the integrations over $l(x)$ for the longitudinal waves, and over $l(x)$ and δl for the transverse waves, we find that in both cases the velocity is of the form

$$v \propto \langle l\rangle\sqrt{\langle k\rangle/m} \tag{7}$$

where $\langle l\rangle$ is the average of $l(x)$, $\langle k\rangle = Ew^2/\langle l\rangle$ for the longitudinal waves, and $\langle k\rangle = Ew^4/\langle l\rangle^3$ for the transverse waves. The prefactors not included in equation (7) are of the order unity in both cases. There are also other factors of order unity that will affect the true velocity. These factors arise from the fact that no fibre segment chain in a random-fibre network will be perfectly straight, and they will therefore be slightly longer than the travelled distance x. It is, however, very difficult to exactly evaluate the effective length of the chains followed by the first displacement maxima. In order to get an expression for the wave propagation velocity as a function of the density of fibres (q) we have to calculate $\langle l\rangle$ as a function of q. $\langle l(q)\rangle$ is easily obtained from the distribution $P(l)$, and the result is $\langle l\rangle = \pi L/2q$ in the limit of high q. By inserting this in $\langle k\rangle = Ew^2/\langle l\rangle$ for the longitudinal waves, and $\langle k\rangle = Ew^4/\langle l\rangle^3$ for the transverse waves, and using equation (7), we finally arrive at the wave-propagation velocity

$$v = \kappa\sqrt{\frac{\pi Ew^2L}{2qm}} \tag{8}$$

where $\kappa = f_{gl}$ for the longitudinal waves, and $\kappa = f_{gt}2qw/\pi L$ for the transverse waves. f_{gl} and f_{gt} are the proportionality factors of order unity for the longitudinal and transverse waves, respectively.

The amplitude decay in a one-dimensional chain will mainly take place at the interfibre crossings, where the segment chain changes direction. The change in the direction is more or less an uncorrelated non-uniform random variable, which means that we can use an effective angle of direction change to describe the ensemble [9]. Since our model is linear, we expect that the amplitude will be decreased by a constant fraction (γ) at each crossing. In other words, the amplitude ($A(x)$) decay in the segment-chain model will be governed by

$$\frac{\mathrm{d}A(x)}{\mathrm{d}x} = -\gamma A \tag{9}$$

which has a simple exponential solution, $A(x) = A_0\exp(-\gamma x)$. This exponential decay has been verified and analysed in more detail for the random spring network [9].

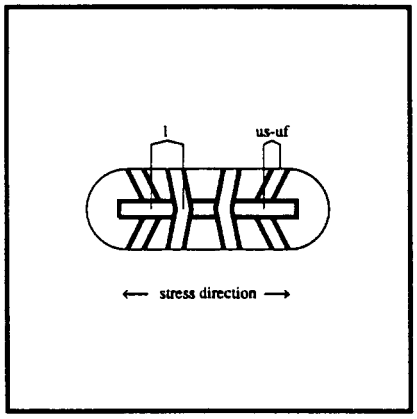

Figure 3. A schematic description of the Cox model. The segment length l and the displacement difference $u_s - u_f$ are indicated in the figure.

4. The effective medium model

In the above model we considered networks for which either the bending or the axial modulus was much smaller than the other. The wavelength was also relatively short. In the opposite limit, i.e. when the bending and axial moduli are about the same, and the wavelength is long, we expect that the fibre network will act as an effectively continuous and homogeneous medium (cf figure 1). In such a case the velocity of elastic waves depends on the effective Young's modulus (E_n), the Poisson ratio (σ), and the effective mass density (ρ) of the network. The effective mass density of our network is $\rho = m/\langle l\rangle^2$. The coefficient of unilateral compression is defined as $C = E_n/(1-\sigma^2)$, and the shear modulus as $G = E_n/2(1+\sigma)$. These two factors (C, G) can be calculated for fibre networks within the effective medium approximation introduced by Cox [2]. The Cox model for the stress distribution in the fibres of a network is based on force balance in the fibre–fibre crossings. Force balance means that a change in the stress along a fibre across a crossing is equal to the stress applied to the crossing by the intersecting fibre. The Cox model then views each single fibre as connected to an elastic sheet (the rest of the network) via the segments of the crossing fibres (figure 3). If the displacements in the sheet are denoted by $u_s(x)$, and the displacements in the fibre by $u_f(x)$, the stress (σ_f) in the fibre cross section as a function of the position (x) along the fibre is given by

$$l\frac{\mathrm{d}\sigma_f}{\mathrm{d}x} = c\frac{(u_f - u_s)}{l} \tag{10}$$

where c is a stress-transfer constant ($l_i = l$ is assumed to be constant in the model). As the stress and strain are related through $\sigma = E\epsilon$, and the displacements can be expressed as $\mathrm{d}u_s/\mathrm{d}x = \epsilon_s$ and $\mathrm{d}u_f/\mathrm{d}x = \epsilon_f$, it is easy to verify that the Cox expression

$$\sigma_f(x,\hat{c}) = E\epsilon_s\left[1 - \frac{\cosh(\hat{c}(1/2 - x/L))}{\cosh(\hat{c}/2)}\right] \tag{11}$$

where $\hat{c} = \sqrt{c}L/l$ is a solution of equation (10) satisfying the boundary conditions $\sigma_f(0,\hat{c}) = \sigma_f(L,\hat{c}) = 0$. In the Cox model stress correlations over more than one segment length in the intersecting fibres are neglected. Therefore, c is a function of only w/l and not of w/L.

In the absence of a transverse Poisson contraction of the network, the angular dependence of the axial stress is simply given by

$$\sigma_f(x, \hat{c}, \theta) = \sigma_f(x, \hat{c}) \cos^2(\theta) \tag{12}$$

where θ is the angle between the fibre and the direction of the external tension. The elastic energy stored in the network (as an axial tension of the fibres) is $\frac{1}{2}\int_V \sigma\epsilon \, \mathrm{d}V$, where integration is over the area of all fibre segments in the two-dimensional network (most of the elastic energy in a random-fibre network is stored as an axial tension of the fibres [14]). Using equations (11) and (12), the elastic energy of the network can be written as

$$W(\hat{c}) = \frac{1}{2} E \epsilon_s^2 L_x L_y q \frac{w^2}{L^2 \pi} \int_{-\frac{\pi}{2}}^{\frac{\pi}{2}} \int_0^L \cos^4(\theta) f^2(x, \hat{c}) \, \mathrm{d}x \, \mathrm{d}\theta \tag{13}$$

where $f(x, \hat{c})$ is the expression inside the brackets in equation (11), $L_x L_y$ is the size of the network and w the width of the fibres. The total elastic energy in the network can also be written as $W = (L_x L_y/2) E_n \epsilon^2$, where E_n is the effective Young's modulus of the network. By combining this equation with equation (13), we arrive at an expression for C and G,

$$C = a \frac{3 E w^2}{8L} (q - b q_c) \tag{14}$$

where q_c is the percolation critical density, and a, b are constants. A similar expression is found for G with different values for the constants a and b. The velocities of elastic waves in a homogeneous medium are simply $\sqrt{C/\rho}$ for the longitudinal waves, and $\sqrt{G/\rho}$ for the transverse waves. Using equation (14) we find that

$$v = \sqrt{\frac{\pi E w^2 L}{2qm}} \sqrt{\frac{3a\pi}{16}} \sqrt{1 - b\frac{q_c}{q}}. \tag{15}$$

The correct values of the parameters a and b cannot be determined by the Cox model [7]. To get the values of these parameters we used a finite-element code [7], and obtained the following values for networks with the same parameter values as the ones used in the simulations to be described in the next section: $a \approx 1.08$, $b \approx 2.8$ for the longitudinal waves, and $a \approx 0.35$, $b \approx 3.3$ for the transverse waves. We notice in passing that these values give the Poisson ratio $\sigma = 0.35$.

In a continuous and homogeneous medium the amplitude of the first displacement maximum would remain constant. In a discrete but homogeneous medium the amplitude will decrease due to dispersion. The dispersion relation for discrete mass points coupled by harmonic potentials will lead to a power-law decay at late times for the amplitude: $A(x) \propto x^{-1/3}$ [15].

5. Numerical results

We have used the numerical model described in section 2 to test the two model solutions, i.e. equations (8) and (15). At first we test the one-dimensional model. In figure 4 the distances along the x-axis of the crossing points are plotted against the average time of arrival of the first displacement maximum at these points for varying values of the network parameters (i.e. E, q, m, L, w). In order to test equation (8), the scale is set for each curve separately so that they should collapse on one velocity curve for the transverse and on another for the longitudinal waves. This means that the scale is determined by $\sqrt{\pi E w^2 L/2qm}$ for the longitudinal waves, and by $\sqrt{2qEw^4/\pi mL}$ for the transverse waves. It is obvious that the scaling works quite well with respect to E and m for the longitudinal

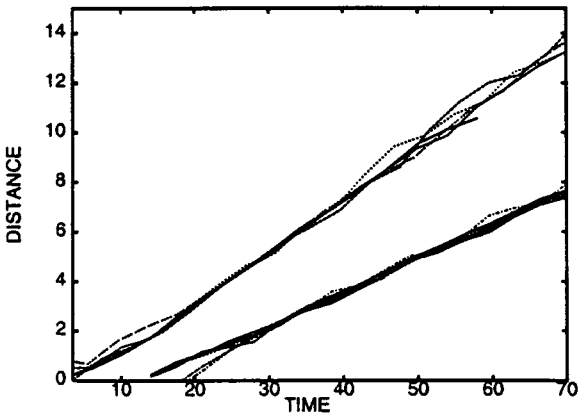

Figure 4. Velocities of transverse and longitudinal waves (slopes of the curves). For the transverse waves (lower curves) $q/q_c = 4, 6, 8$, $m = 0.01, 0.05, 0.1$, $w = 0.07, 0.1, 0.15$ and $l_f = 2, 3$. For the longitudinal waves (upper curves) $q/q_c = 4$, $w = 0.01$, $l_f = 2$, $m = 0.0005, 0.0001, 0.000\,02$, and $E = 3, 1, 0.3$.

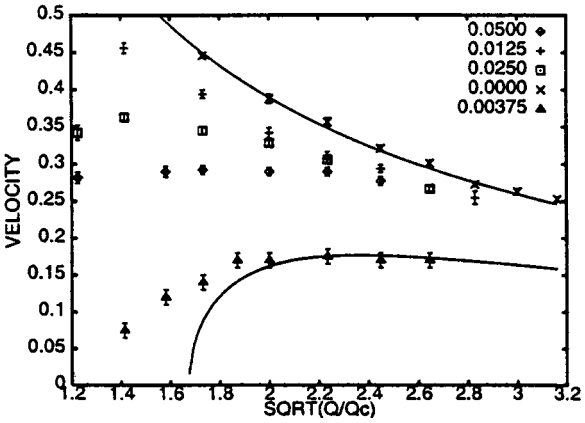

Figure 5. Velocities of longitudinal waves as a function of $\sqrt{q/q_c}$. The velocities are scaled by $\sqrt{\pi E w^2 l_f/2m}$. The upper line is given by equation (8), and the lower line by equation (15). Simulation data for $w/l_f = 0.05, 0.025, 0.0125, 0.003\,75$ and for spring networks ($w/l_f \to 0$) are displayed ($f_{gl} = 0.97$). The frequency is 0.125, except for $w/l_f = 0.003\,75$ in which case it is 0.0125.

waves. We found, however, that scaling is not fulfilled with respect to w, L or q. This indicates that both modes (equations (8) and (15)) are included in the observed velocity (b has been found to depend on w/L [6]). For the transverse waves scaling works with respect to all parameters E, m, w, L and q, which indicates that velocity is dominated by the segment-chain mode (equation (8)). Figure 4 also indicates that the velocities (slopes of the curves) remain fairly constant, only at short times can a boundary effect be observed.

In order to further analyse the longitudinal waves, we plot in figure 5 their velocities, scaled by $\sqrt{\pi E w^2 L/2m}$, for different fibre widths as a function of density. It is evident that the velocities are in excellent agreement with equation (8) for slender fibres, while they approach equation (15) for thick fibres. For very low frequencies the velocity is accurately

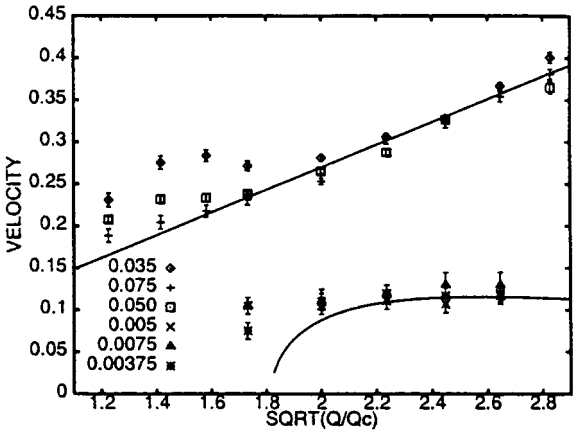

Figure 6. Velocities of transverse waves as a function of $\sqrt{q/q_c}$. The upper line is given by equation (8), and the lower line by equation (15). Simulation data for $w/l_f = 0.075, 0.05, 0.035$ were obtained using the frequency 0.125 (these data are scaled by $\sqrt{\pi E w^2 l_f/2m}$). The rest of the data, $w/l_f = 0.0075, 0.005, 0.003\,75$, are for a frequency of 0.0125 (these data are scaled by $\sqrt{2Ew^4/\pi m l_f}$); $f_{gt} = 1.0$.

determined by equation (15) even for slender fibres. The only deviation is close to the critical density of percolation where the Cox model fails. Figure 5 demonstrates clearly that there is a cross-over phenomenon between the two model solutions as the fibre width is changed.

In figure 6 similar results are shown for the transverse waves scaled by $\sqrt{2Ew^4/\pi mL}$. From this figure it is evident that the segment-chain model describes the situation for relatively broad fibres ($w = 0.035, 0.05, 0.075$) and at high densities. At small densities, however, the velocity deviates from the segment-chain model prediction. Deviation begins at densities for which the longitudinal mode is about 20% faster than the transverse mode (at $\sqrt{q/q_c} = 1.6, 1.9, 2.3$ in figure 6). It is obvious that at these points the longitudinal mode begins to dominate the first displacement maximum even though the driving source operates in the transverse mode. A corresponding phenomenon was also observed for the longitudinal waves at high densities and for thick fibres (i.e. for densities higher than those shown in figure 5). Numerically, the effective medium velocity was difficult to find for the transverse mode, but for very low frequencies (0.0125) and slender fibres (0.0075, 0.005, 0.0035) it could be detected. Notice that these velocities are scaled according to equation (15), i.e. the scale is given by $\sqrt{\pi E w^2 L/2m}$. This case is different from the other data points in the figure 6 which are scaled by $\sqrt{2Ew^4/\pi mL}$.

In order to clarify the effect of the rate at which the signal changes, we have analysed the velocities for a varying driving frequency. This complements the results shown in figures 4 and 5. For wavelengths which are of the same order of magnitude as the average segment length $\langle l \rangle$, the network cannot reach a local equilibrium while the first displacement maximum is passing by. This means that the segment-chain model is expected to give the correct velocity. As the frequency is lowered, the velocity should approach that of the effective-medium model. This is indeed what seems to happen as is evident from figure 7. The results in this figure are for longitudinal waves and the parameters are $q/q_c = 3$, $m = 8.14 \times 10^{-8}$, $w = 0.0001$ and $L = 2$.

It is obvious that for any driving frequency both the segment-chain and effective-medium

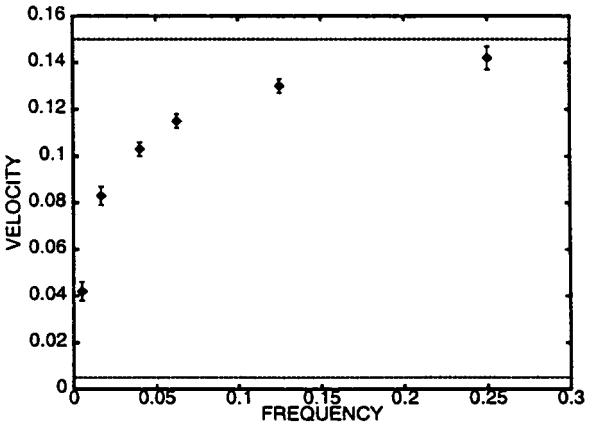

Figure 7. The observed longitudinal velocity without mode distinction as a funtion of frequency; $q/q_c = 3$, $m = 8.14 \times 10^{-8}$, $w = 0.0001$ and $l_f = 2$. The wavelengths are $0.6l_f, 1.0l_f, 1.8l_f, 2.6l_f, 5.1l_f, 8.4l_f$, which correspond to the frequencies $\frac{1}{4}, \frac{1}{8}, \frac{1}{16}, \frac{1}{25}, \frac{1}{60}, \frac{1}{200}$, respectively. The upper and lower lines are the segment-chain model velocity and the effective-medium velocity, respectively.

modes are always excited in the random-fibre network. If it is not possible to distinguish between these modes, which is certainly the case at short distances, the observed velocity will have an apparent dependence on the driving frequency as demonstarted in figure 7. The relative importance of the modes depends on the driving frequency and on the fibre stiffness as described above. As the segment-chain modes are exponentially decaying (cf figure 8), at late times the propagating signal will always be dominated by the effective medium modes. In fact distinction between these two kinds of modes is much easier in randomly diluted lattices where they both also appear. Results for these systems will be published elsewhere [15].

Finally, the two models were tested by following the amplitude as a function of distance, and the results are shown in figure 8. The predicted cross-over from a power-law decay (or an almost constant amplitude) for broad fibres to an exponentially decreasing amplitude for slender fibres is obvious. Note that the exponential decay is very fast for the spring networks ($w = 0.0$). The penetration depth of the wave is for these networks at most a few fibre lengths [9].

6. Discussion

By comparing equations (8) and (15) it is evident that the velocity of the segment-chain model and that of the continuum model are different. For the longitudinal waves this difference essentially arises from the parameter b, and for the transverse waves it is even more pronounced. For the transverse waves the result of the one-dimensional model scales as $\sqrt{2qEw^4/\pi mL}$, while that of the effective-medium model scales as $\sqrt{\pi qEw^2L/2m}$. In the effective-medium model b arises from the distribution of stress along individual fibres, which in this case is an equilibrium distribution [6]. In the one-dimensional model there is no equilibrium and b does not appear.

It is evident that not only the velocities but also the effective Young's moduli of the two models described above are different because local equilibrium is achieved in one model but not in the other (here we mean the Young's modulus as determined from the velocity of the

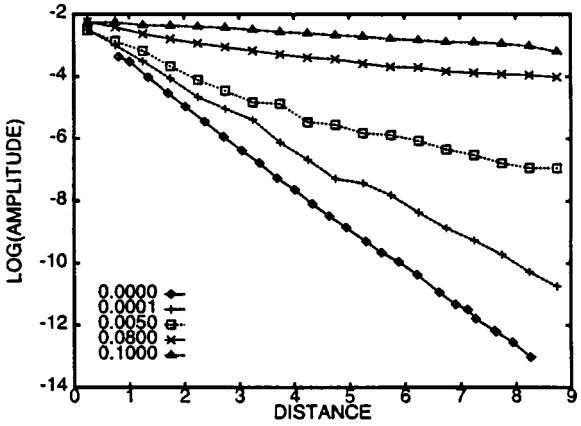

Figure 8. Logarithm of the amplitude of the first displacement maximum as a function of distance from the driving source. The fibre widths are $w = 0.0, 0.0001, 0.005, 0.08$, and 0.1.

waves). We would therefore expect that, for high-frequency ultrasound, the model of non-interacting segment chains should give the observed effective Young's modulus, while the continuum model should give the observed value as the frequency becomes small (cross-over should take place when the wavelength is of the order of a few l). This difference between the 'dynamic' and 'static' moduli is actually seen in experiments on paper sheets [16], but there may be other factors (i.e. viscoelasticity) which explain this difference as the frequency of the ultrasound used in the experiments was rather low. Recent experiments [17] that also apply low-frequency ultrasound, indicate that equation (15) fits well the observed velocity for fairly low values of q when paper sheets can still be considered as two-dimensional. Notice that a low q does not here mean a q close to the critical threshold of percolation, but rather a q low compared with that of ordinary paper. The same experiments also gave a value 0.58 for the ratio of the transverse and longitudinal velocities. This means that the observed Poisson's ratio is $\sigma = 0.33$, which agrees with the value found from the effective-medium model, $\sigma = 0.35$. Attenuation of the segment-chain mode makes its detection difficult.

Many earlier studies [10, 18] have dealt with localization, which is related to the long-time behaviour of the energy carried by the elastic waves. Localization is a result of interference between incoming and scattered waves. Here we consider only the very first wavefront (no interference with backscattered waves). In the effective-medium limit it is quite obvious that the first displacement maximum is dominated by propagating modes, at least on short scales, and that localized modes such as fracton type modes in percolating lattices [18] are not important. On scales very much larger than those used in the simulations, localization could perhaps be seen, although it may be beyond the present computational capabilities. In the limit of a small bending stiffness of the fibres (i.e. the limit of the one-dimensional model), the situation is more complicated. The exponentially decaying amplitude is in this case a consequence of the fact that the slower modes are being left behind the first displacement maximum at the interfibre crossings (cf equation (9)) [9]. Localization, which is governed by a different mechanism, will also in this case take place in a larger length scale. When the bending stiffness is exactly zero (i.e. a spring network), however, only zero-frequency and localized modes exist [9].

In a sense the random-fibre networks analysed here resemble granular materials [19]. All mass is concentrated on the 'grains' of the interfibre crossings, and the fibre segments

correspond to the interactions between the grains. An important difference is that all 'collisions' between 'grains' are now elastic, which means that no elastic energy is lost into heat in the fibre networks. Another important difference is of course that the interactions in the fibre network make large displacements impossible. There are, however, also a few similarities. For instance, it has been demonstrated that much of the stress in granular materials is concentrated along strings [20] which resemble the one-dimensional paths of the transient signals in the fibre network.

To conclude, we have shown that there are two kinds of modes of 'elastic' waves in random-fibre networks, and that these modes can be understood within simple models. They depend differently on the parameters of the network. The segment-chain mode dominates the velocity at short distances of longitudinal (transverse) waves in networks where the axial (bending) stiffness of the fibre segments dominates, especially in the limit of high frequencies. There also appears an apparent frequency dependence in the observed velocities if the modes cannot be distinguished. Furthermore, there should be a difference in the elastic moduli obtained from dynamic and static measurements. Dynamic means here frequencies higher than those related to the average fibre length. The difference between the segment-chain behaviour and the effective-medium behaviour is particulary pronounced in the case of transverse modes.

Acknowledgment

We thank V Räisänen for useful discussions.

References

[1] For reviews see for example Herrmann H J and Roux S (ed) 1990 *Statistical Models for the Fracture of Disordered Media* (Amsterdam: North-Holland)
Sahimi M and Arbabi S 1993 *Phys. Rev.* B **47** 695
Arbabi S and Sahimi M 1993 *Phys. Rev.* B **47** 703
[2] Cox H L 1952 *Br. J. Appl. Phys.* **3** 72
[3] Page D H and Seth R S 1980 *Tappi J.* **63** 113
[4] Ramasubramanian M K and Perkins R W 1988 *J. Eng. Mater. Technol.* **110** 117
[5] Åström J A and Niskanen K J 1993 *Europhys. Lett.* **21** 557
[6] Åström J, Saarinen S, Niskanen K and Kurkijrvi J 1994 *J. Appl. Phys.* **75** 5
[7] Räisänen V I, Alava M J, Niskanen K J and Nieminen R M 1997 *Report* 240 Laboratory of Physics, Helsinki University of Technology (Helsinki: Otakustantamo)
[8] Räisänen V I, Alava M J, Niskanen K J and Nieminen R M 1996 *Nord. Pulp Paper Res. J.* **11** 243
[9] Kellomäki M, Åström J and Timonen J 1996 *Phys. Rev. Lett.* **77** 2730
[10] For reviews see for example Sheng P 1995 *Introduction to Wave Scattering, Localization, and Mesoscopic Phenomena* (San Diego, CA: Academic)
Faris W G //www.ams.org/publications/notices/199508/faris.html
[11] Pastur L and Figotin A 1992 *Spectra of Random and Almost-periodic Operators* (Berlin: Springer)
[12] Stauffer D 1985 *Introduction to Percolation Theory* (London: Taylor and Francis)
[13] Arfken G 1985 *Mathematical Methods for Physicists* (San Diego, CA: Academic)
[14] Hamlen R C 1991 *PhD Thesis* University of Minnesota
[15] Åström J, Kellomäki M, Alava M and Timonen J 1997 *Phys. Rev.* E to appear
[16] Nordell E 1992 *Masters Thesis* Kungl. Tekniska Högskolan, Stockholm
[17] Aalto M, Kellomäki M, Åström J, Niskanen K and Timonen J unpublished
[18] Mukherjee S, Nakanishi H and Fuchs N H 1994 *Phys. Rev.* E **49** 5032
[19] Jaeger H M, Nagel S R and Behringer R P 1996 *Rev. Mod. Phys.* **68** 1259
[20] Liu C H, Nagel S R, Schecter D A, Coppersmith S N, Majumdar S, Narayan O and Witten T A 1995 *Science* **269** 513